RCMOS – Multidisciplinary Scientific Journal of Knowledge.
ISSN: 2675-9128. São Paulo-SP.

Year V, v.1 2025. | submission: 08/15/2025 | accepted: 08/17/2025 | publication: 08/19/2025

Structured CNF nanocomposites using CNC as a mechanical reinforcing agent

Nfc nanocomposites structured using CNC as mechanical agent for reinforced strength properties

Renato Augusto Pereira Damásio1 - SUNY College of Environmental Science and Forestry, Syracuse, USA
Cicero Pola2 – Iowa State University, Ames, USA
Fernando Jose Borges Gomes3 - Federal Rural University of Rio de Janeiro, Seropedica, Rio de Janeiro, Brazil
Elenice Maia4 – PhD in Forest Science, Suzano, Americana, São Paulo, Brazil
Jorge Luiz Colodette5 - Emeritus at University of Viçosa, Viçosa, Minas Gerais, Brazil

ABSTRACT: The development of film-forming nanocomposites from nanofibrillated (CNF) and nanocrystalline (CNC) cellulose is a sustainable alternative for application in numerous industrialized materials due to their differentiated mechanical and optical characteristics. The objective of this study was to evaluate the potential of CNF and CNC in the production of transparent nanocomposites with high mechanical strength. The CNF-CNC nanocomposites were produced using the *casting technique,* using CNF as the polymeric dispersion matrix for different dosages of CNC as mechanical reinforcement. The polymeric base used for CNF employed 10 g/m² of this nanocellulose in its suspended form, while CNC was applied at doses of 3; 6; and 12%, after its suspension in water. The addition of cellulose nanocrystals allowed a reduction in the surface roughness of the produced nanocomposites.

The ultimate tensile strength increased by 103% and 287% for the 3% and 12% CNC applications, respectively, while the elastic modulus increased by 591% for the 12% CNC dose. Tensile strength increased by 61% with the addition of 12% CNC. Similarly, the physical properties of weight and apparent specific volume showed significant improvements. The incorporation of CNC allowed a reduction in opacity of up to 53%, with consequent gains in transparency of the nanocomposites. The nanocomposites containing CNC showed greater thermal stability, with lower mass loss, than the reference containing only CNF. The incorporation of CNC into the CNF polymer base in the formation of nanocomposites with high mechanical strength and transparency is a viable technological alternative.

Keywords: Nanocrystalline cellulose, nanofibrillated cellulose, nanocomposites, nanofilms.

ABSTRACT: The development of nanocomposites forming films from nanofibrillated cellulose (NFC) and nanocrystalline cellulose (CNC) present as a sustainable alternative for application in many industrial materials, due to their different mechanical and optical characteristics. Thus the aim of this study was to evaluate the potential of NFC and CNC in the production of transparent nanocomposites with high mechanical resistance. The NFC-CNC nanocomposites were produced according to casting technique, using as the polymeric matrix CNF dispersion for different dosages CNC as mechanical reinforcement. The base polymer NFC used 10 g/m² for this nanocellulose that in its suspended form as CNC was applied in doses of 3%, 6% and 12% after suspension in water. The addition of cellulose nanocrystals allowed

[1]PhD Student, Department of Chemical Engineering, SUNY College of Environmental Science and Forestry, Syracuse, United States – damasiorenato@gmail.com - http://lattes.cnpq.br/9704098989769768 - https://orcid.org/0000-0001-7268-2774

the reduction of the surface roughness of the resulting nanocomposites. The maximum load increased 103 and 287% for CNC applications 3 and 12% respectively. While the modulus increased 591% to 12% of the dose CNC. The tensile strength increased from 61% with the addition of 12% CNC. Likewise, the physical properties of apparent specific volume and weight showed significant gains. Due to CNC incorporation allowed reducing the opacity to 53% with consequent increased in transparency of nanocomposites. Nanocomposites containing CNC showed higher thermal stability with less weight loss compared to references containing only CNF. The CNC incorporated into the NFC polymeric matrix, results in the nanocomposite formation with high strength and transparency, is a viable alternative technology.

Keywords: Nanocrystals, nanofibrillated cellulose, nanocomposites, nanofilms.

1. INTRODUCTION

The use of biopolymers has been an important alternative to fossil-based materials, such as plastics, in the production of nanocomposites (ESPITIA et al., 2013). Therefore, plant fibers have become the target of the modern biorefinery industry, since their composition includes a series of structural chemical components of great interest for use in the formulation and constitution of various new products.

However, most biopolymers used in the manufacture of composites and nanocomposites generally have lower mechanical strength than polymers of non-natural origin (TUNC & DUMAN, 2011). Recent advances in the use of tools such as nanotechnology allow the use of biopolymers, as well as their production and dispersion in various matrices, with the aim of increasing the mechanical strength properties of the material. Recently, many researchers have begun to apply cellulosic fibers as a filler or reinforcement phase, instead of synthetic fibers (JOSHI et al., 2004), due to their biodegradability, lighter weight, lower cost, greater rigidity and strength (GEORGE et al., 2001; LI et al., 2007; DUFRESNE, 2010; KHALIL et al., 2014).

Nanocelluloses (CNC and CNF) are nanoparticles that can be used in a series of technological applications, in order to promote modifications in the physical structure of the material that induce gains in mechanical resistance and transparency to the matrix to which they are applied.

Nanocomposites are generally multiphase products, in which at least one phase is composed of particles with a nanometric dimension, in the range of 1 to 100 nm (MANOCHA et al., 2006). The properties of nanocomposites depend on the nature of the polymer matrix, the interaction between the matrix and the nanoparticles, and the interface structure between the nanoparticles and the large elements (RAMAZANOV et al., 2010). Composites containing nanoreinforcements have a larger surface area and fewer defects (SEYDIBEYOGLU & OKSMAN, 2008).

CNF and CNC are nanocelluloses that have the ability to percolate and intertwine when well dispersed in the matrix in which they are applied. The physical phenomenon of approximation occurs due to the formation of hydrogen bonds (NAKAGAITO et al., 2009).
The formation of these bonds ensures greater interaction between the matrix and the nanocelluloses, thus increasing the material's mechanical strength. Furthermore, according to Yu et al. (2006), the natural hydrophilic nature is a major advantage for the development of composites based on water-miscible materials, such as cellulose derivatives.

The objective of this study was to evaluate the potential of CNF and CNC in the production of transparent nanocomposites with high mechanical strength. To this end, the nanocomposites (CNF-CNC) produced using these nanocelluloses were fully characterized. The growing use of biopolymers with characteristics capable of replacing synthetic polymers motivated the production of the nanocomposites characterized in this study, which can be applied in the composition of electronic equipment and special coatings for food and transparent packaging.

2. MATERIAL AND METHODS

2.1 Material

CNF and CNC nanocelluloses were used in this study to produce a differentiated, nanostructured, and transparent nanocomposite. Cellulose nanocrystals from the original pulp of a *mix* of coniferous species were also used in this study. The CNCs used here were provided by the *United States Department of Agriculture* (USDA).
- *Forest Products Laboratory.* The original nanofibrillated cellulose from industrial bleached hardwood pulp was sourced from a pilot plant of a traditional Brazilian pulp and paper company.

2.2 Work plan

Figure 1 illustrates the steps performed in this study, from nanocomposite production to their complete characterization. After the CNF-CNC nanocomposites were produced, they were characterized in relation to their (1) morphological characteristics, (2) their mechanical and optical characteristics, and (3) their thermal characteristics.

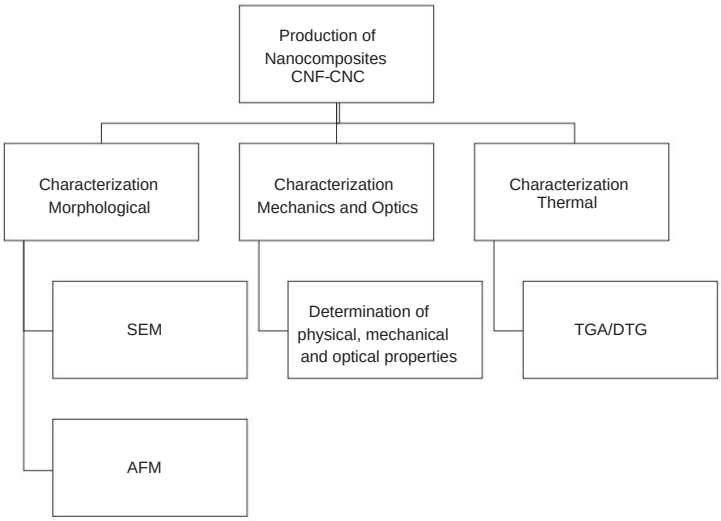

Figure 1 – Flowchart of the work plan for this study.

2.3 Production of CNF-CNC nanocomposites

The diagram illustrated in Figure 2 exemplifies how the nanocomposites were produced in this study, using the *casting technique,* in order to evaluate the potential for mechanical reinforcement offered by different CNC dosages applied in their composition. The variable CNC dosages (0, 3, 6, and 12% w/w) were used together with 10 g/m² of CNF, to make the nanocomposite in the forming plate (Table 1).

Table 1 – Proportions of nanocelluloses used to make CNF- nanocomposites
CNC

Treatment	CNF	CNC
T0	10 g/m²	0%
T1	10 g/m²	3%
T2	10 g/m²	6%
T3	10 g/m²	12%

The *freeze-dried* CNC and CNF suspensions were subjected to mechanical agitation for a 10-minute reaction time in a beaker. To improve and ensure that the nanocrystals used were fully dispersed in the medium, 100 mL of distilled water was added to each beaker containing the mass ratio of CNC used in each treatment, relative to the chosen CNF weight (Table 1). After the initial preparation of the required mass quantity of both nanocelluloses and their reaction time completed, the mixture was poured into Petri dishes to begin drying. Drying conditions followed a temperature of 30 ± 1 °C for 72 hours, using the *casting* technique to form the nanocomposites.

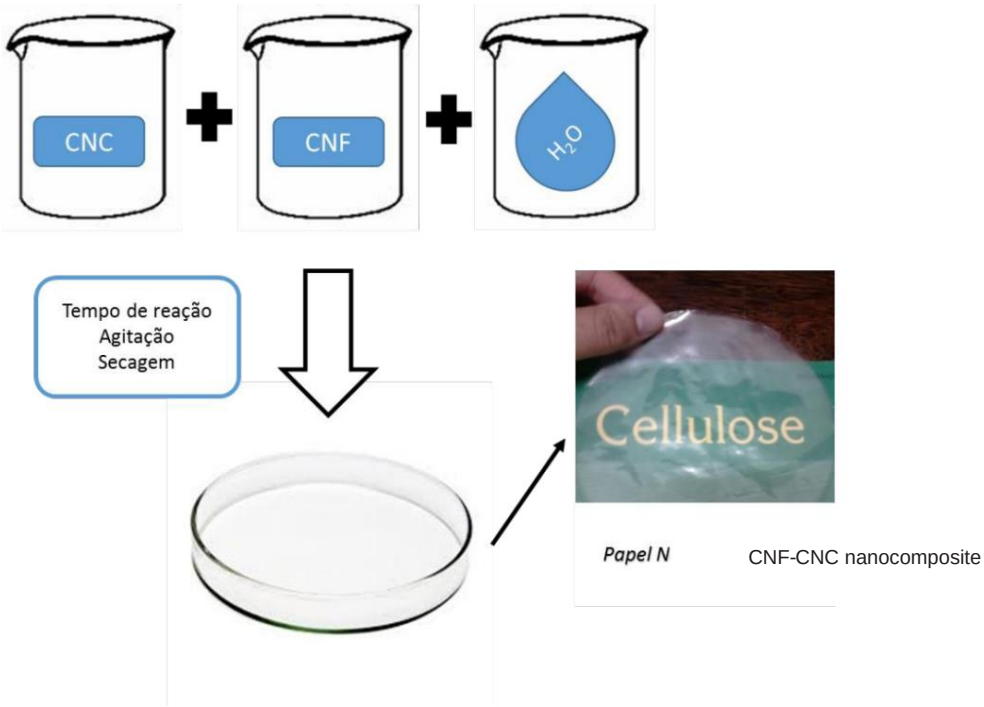

Figure 2 – Production of structured CNF-CNC nanocomposites.

2.4 Scanning electron microscopy (SEM)

The dried samples were mounted directly on *stubs* and metallized in a model FDU-010 metallization equipment, Balzers, Germany, coupled to a model SCA-010 cathodic sputtering set. The material was observed in an electron microscope model LEO 1430 VP (Zeiss, Germany), from NMM-UFV.

2.5 Atomic force microscopy (AFM)

Atomic force microscope measurements of the studied CNF-CNC nanocomposites were performed at the Physics Department of the Federal University of Viçosa-MG, Brazil. The topography of the nanocomposites was studied using atomic force microscopy (AFM, NT-MDT, Russia). Furthermore, the roughness of the produced films was calculated using NOVA 1.0.26.1443 *software* . AFM images were acquired in an intermittent contact mode in random areas of 50 × 50 μm². The samples were analyzed at room temperature (25 ºC).

2.6 Physical, mechanical and optical properties

After the preparation and acclimatization of the CNF-CNC nanocomposites, the optical, physical and mechanical properties were determined according to the analytical procedures described in Table 2.

The mechanical properties of the developed nanocomposites were determined by the standard ASTM D882-09 method (ASTM, 2009), which was adapted using a model of

Instron 3367 universal testing machine *(Instron Corporation,* Norwood, MA, USA), equipped with a 1 kN load cell. The CNF-CNC nanocomposite samples were cut into rectangular strips (100 × 15 mm). The initial separation between grips was 100 mm, and the crosshead speed was set at 25 mm/min. This test was repeated several times for each treatment to confirm its reproducibility.

Table 2 – Analytical procedures for characterizing the produced nanocomposites

Parameters	**Procedures**
Thickness	T551 om-06
Grammage	T410 om-08
Apparent specific gravity	T220 sp-01
Apparent specific volume	T220 sp-06
Tensile index, specific modulus of elasticity, maximum load and elongation - Adaptation	ASTM D882-09
Opacity and Transparency	T1214 sp-07

2.7 Thermal analysis

The analysis was performed using a thermogravimetric analyzer (TGA-1000, Navas Instruments, Conway, SC, USA). The CNF-CNC nanocomposite samples (approximately 1 g) were heated from 25 to 700 °C at a heating rate of 10 °C/min under a nitrogen atmosphere. The weight losses of the samples were measured as a function of temperature. The second curve (DTG) was generated from the first derivative of the mass loss, which allows the determination of the *onset,* maximum, and *endset* temperatures to characterize the thermal degradation events.

2.8 Statistical analysis

Statistical analyses of the results of physical, mechanical, and optical tests of nanocomposites produced using different levels of CNC addition were performed using RStudio *software* version 3.1.2. Graphs were plotted using *SigmaPlot* 11.0 software.

To evaluate the effect of adding cellulose nanocrystals, the results obtained for each nanocomposite property were evaluated using a completely randomized design (CRD). The results were subjected to analysis of variance (ANOVA), and when a significant difference between treatments was found, the means were compared using the *Skot-Knot test,* adopting a significance level of 5%.

3. RESULTS AND DISCUSSION

3.1 Characterization of the surface of CNF-CNC nanocomposites

Figure 3 illustrates SEM and AFM images of the surface topography of the produced CNF and CNC nanocomposites. The SEM images show that as CNC is added to the nanocomposite composition, the surface roughness and T0 decrease. This fact indicates that there is a modification in the organization and structuring of these nanomaterials due to the self-organization potential that cellulose nanocrystals exhibit during nanofilm formation.

According to Habibi et al. (2010), cellulose nanocrystals, when suspended and subjected to continuous removal of the aqueous phase (e.g., evaporation), tend to adopt configurations that minimize existing electrostatic interactions. The self-organization patterns of this nanomaterial begin while suspended and grow with increasing concentration. Therefore, upon initial contact with the CNF present in suspension in the reaction medium, the influence of these organization patterns on the formation of nanofilms is observed. The "fingerprint" exhibited by these patterns persists throughout film formation and allows studies of their differential behavior, which has valuable applications. Important applications include the manufacture of coating components for decorative materials and security documents (because their optical properties cannot be reproduced by printing or photocopying).

When CNC was added to the production of nanocomposites to produce nanofilms with differentiated characteristics, a higher roughness was observed for T0 (320.74 nm); T1 and T2 showed a decrease in this parameter with increases of 3 and 6% CNC addition, resulting in roughness of 42.15 and 33.36 nm. When adding 12% CNC, the roughness increased, compared to T1 and T2, to 130.40 nm. It was observed that the surface topography of the nanofilms is modified with the different CNC concentrations, which can be demonstrated by the change in the surface roughness values. In T3, the addition of 12% nanocrystals may have caused the generation of excess small-sized materials, which caused a slight increase in the average roughness value found for the surfaces.

Excessive nanoparticles in nanocomposite production can lead to the formation of stress points and agglomerates (ESPITIA et al., 2013), as occurred in the nanofilms produced in this study, which contained a higher CNC content. Stress points are regions that are easily ruptured, resulting in a decrease in the mechanical properties of the nanofilm; this behavior can be observed in the determination of the mechanical properties below.

RCMOS – Multidisciplinary Scientific Journal of Knowledge.
ISSN: 2675-9128. São Paulo-SP.

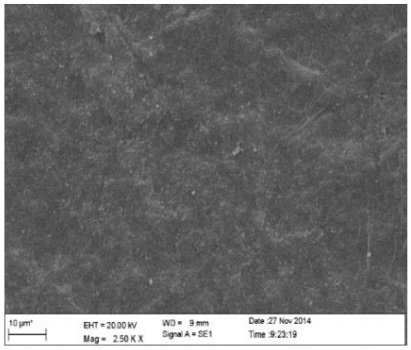

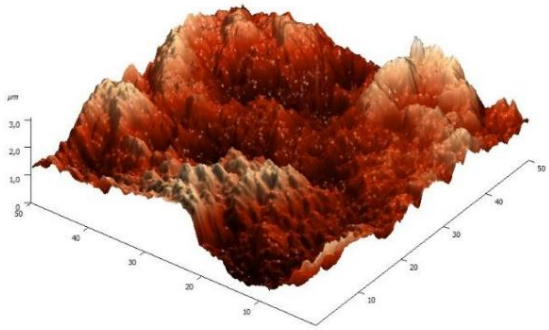

T0

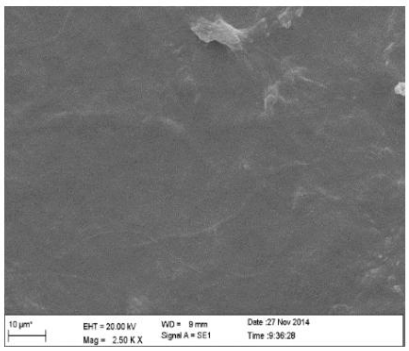

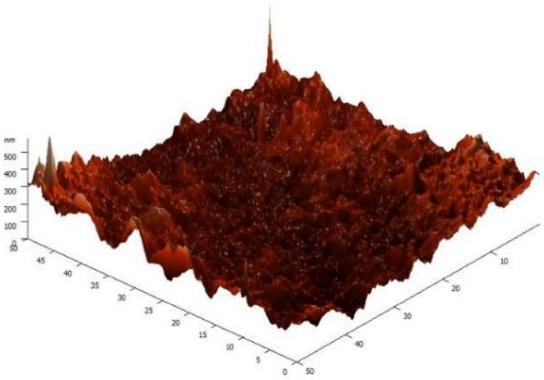

T1

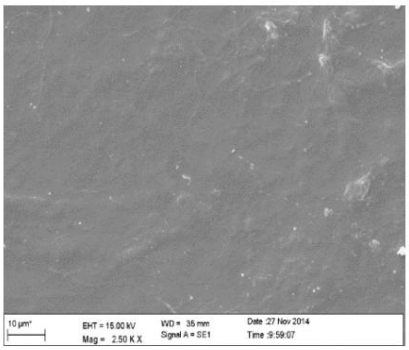

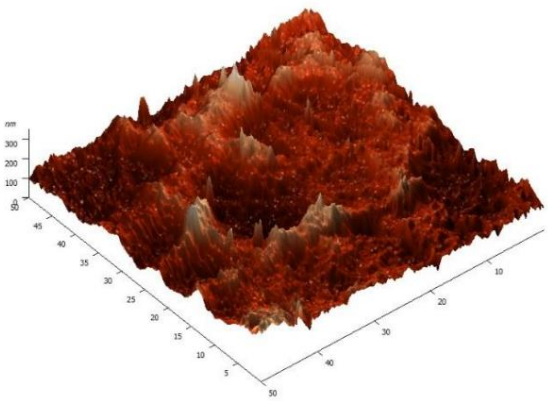

T2

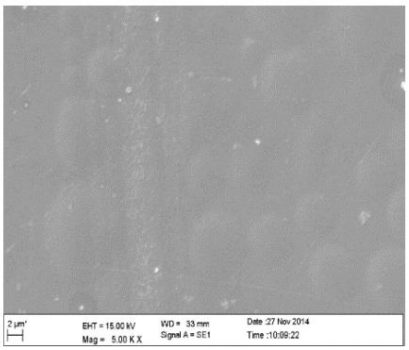

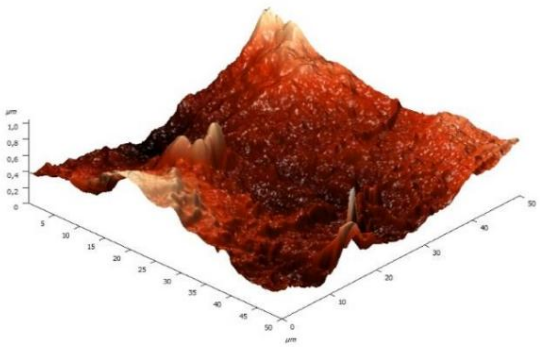

T3

Figure 3 – Scanning electron micrographs on the left and atomic force micrographs on the right of the surface of CNF-CNC nanocomposites, where T0 (0% CNC), T1 (3% CNC), T2 (6% CNC) and T3 (12% CNC).

3.2 Physical-mechanical strength of nanocomposites

The following graphs describe the effect of CNC addition in the studied proportions (0, 3, 6, and 12%) on the physical and mechanical properties of CNF-CNC nanocomposites produced in a CNF matrix. These properties are parameters for controlling and evaluating the quality of nanomaterials for different end applications of this nanocomposite material.

According to Chun et al. (2011), the addition of a new component with a large surface area due to its size allows a large number of bonds to occur at the interface of the CNF-CNC percolation matrix during the CNC incorporation reaction, which better distributes the stress generated by the CNF-CNC network. These bonds, such as intermolecular interactions, significantly influence the physical and mechanical strength properties.

Figures 4a and 4b demonstrate that as the percentage of CNC in the nanocomposite composition increases, the apparent specific weight (ASP) increases in its average values, while the apparent specific volume (ASV) decreases. When adding CNC to the CNF matrix to form nanocomposites, the number of intermolecular interactions and the percolation phenomenon of nanocrystals in the reaction medium containing water and the polymer matrix (CNF) result in a compact structure of the produced nanocomposite.
Therefore, in relation to T0 for apparent specific weight there is an increase of 61; 101; and 156% for T1, T2 and T3, which is inversely proportional to the drop presented by the apparent specific volume, which in relation to T0 results in 38; 51; and 61%, for T1, T2 and T3, respectively.

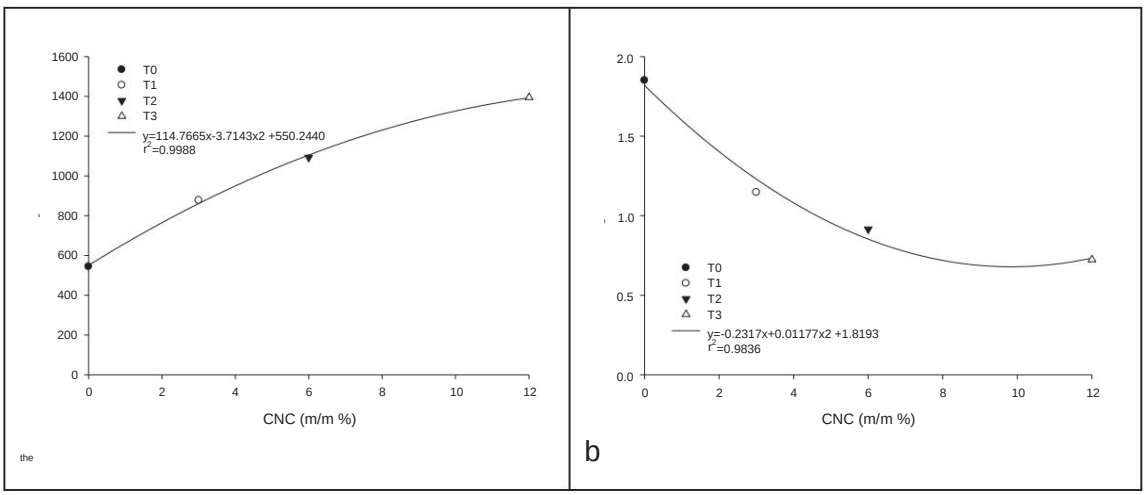

Figure 4 – Behavior of physical and optical properties for the studied treatments, T0 (0% CNC), T1 (3% CNC), T2 (6% CNC) and T3 (12% CNC). a) apparent specific weight and b) apparent specific volume.

Table 3 shows the values found for these properties and that they are all statistically different, which means that the treatments performed have an effect

differentiated. Therefore, the CNC dosage used in CNF-CNC nanocomposites will produce different responses depending on the properties evaluated. In general, there will be gains in strength properties, and greater transparency will be associated with the final material.

Table 3 – Average values of the physical and optical properties of the produced nanocomposite

Treatment	Physical and Optical Properties			
	PEA (kg/cm³)	VEA (cm³/g)	Opacity (%)	Transparency (%)
T0	544.13d	1.85a	10.35a	90.67c
T1	877.42c	1.15b	6.20b	94.54b
T2	1092.90b	0.92c	5.14c	95.54a
T3	1394.62a	0.72d	4.88c	95.82a

* Different letters indicate that the Scott-Knott test, at 5% significance, showed a significant difference between the means. PEA (apparent specific weight) and VEA (apparent specific volume).

Figure 5 shows the behavior of the main mechanical strength properties of the nanocomposites produced, represented by T0, T1, T2 and T3. Among the main properties studied here are the maximum load to rupture (5a), the modulus of elasticity (5b), the elongation to rupture (5c) and the tensile strength (5d).

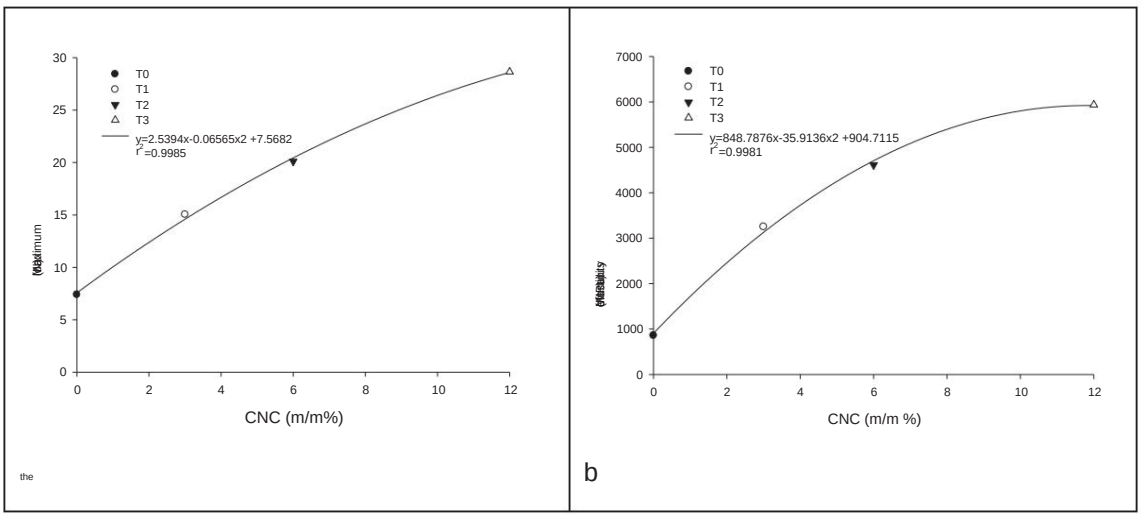

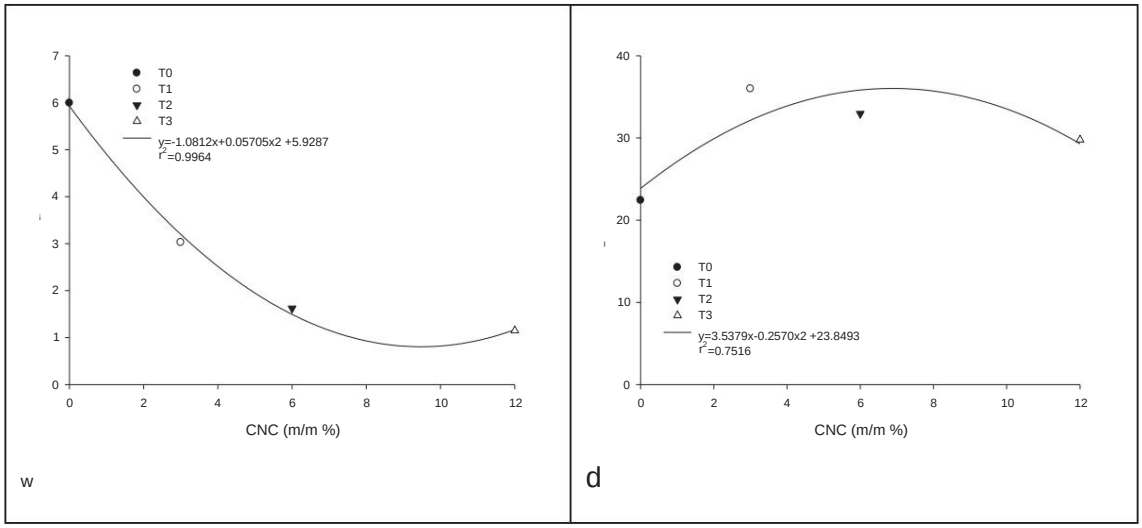

Figure 5 - Behavior of mechanical properties for the studied treatments, T0 (0% CNC), T1 (3% CNC), T2 (6% CNC) and T3 (12% CNC). a) maximum load, b) modulus of elasticity, c) elongation and d) tensile.

The average maximum load supported by the CNF-CNC nanocomposites differed significantly from each other ($p<0.05$), according to the Scott-Knott test. Treatment T3 presented the greater resistance to maximum load, observed in Table 4.

The addition of different amounts of CNC significantly influenced ($p<0.05$) the maximum load supported by the CNF-CNC nanocomposites. Compared to T0, increases of 103 to 287% were obtained for the nanocomposites produced. Some mechanical properties, especially the maximum breaking load, are directly related to the hydrogen bonds formed between the structures, and not necessarily to the strength of the nanocelluloses themselves (ABE & YANO, 2009). Directly proportional to this increase, the modulus of elasticity also showed statistically significant increases in its value. The modulus of elasticity reached gains of over 500% at T3 (12% CNC), when compared to T0. Iwamoto et al. (2007) report that the modulus of elasticity is the property related to the stiffness of materials and that the elasticity of cellulose depends mainly on its crystallinity. The increase in the values of both properties becomes coherent, since in the composition of the nanocomposite matrix the content of nanocrystals, a material with high crystallinity and rigidity, increases considerably.

The rapid growth of these mechanical properties has enabled, with the addition of CNC, the production of highly rigid nanocomposites. Rigidity is an important characteristic to consider in packaging design, and therefore, it must be modified using nanotechnology techniques for its modification and adaptation.

Regarding elongation, when comparing the nanocomposites at T0, it was found that there was a decrease of 49, 73, and 81% for T1, T2, and T3, respectively. This fact can be explained by Iwamoto et al. (2007), who reported lower tensile strength for the films produced, especially for the elongation at break property, due to the excess of components with a lower aspect ratio, which are generally rigid and easily detached from the matrix. It is evident that the treatments with 12% CNC showed a decrease in the tensile and elongation at break values.

Tensile strength is one of the key mechanical properties for evaluating the potential application and use of materials. The nanocomposites produced presented 20.67 MPa for T0, while for the other treatments this value was higher than 26.53 MPa (T4). The nanocomposites produced with 3% and 6% CNC presented the highest values for this property: T1 (39.65 MPa) and T2 (39.66 MPa). Therefore, the dispersion of nanocrystals in the CNF polymer matrix to form the nanocomposites will influence the values of the strength properties, requiring consideration of the dosage at which they will be used.

Table 4 – Average values of the mechanical properties of the produced nanocomposite

Treatment	Mechanical Properties			
	Maximum Load (N)	**Module of Elasticity (Mpa)**	**Elongation (mm)**	**Resistance Tensile (MPa)**
T0	7.40d	858.70d	5.99a	20.67b
T1	15.04c	3250.55c	3.03b	39.65a
T2	20.11b	4612.52b	1.62c	39.66a
T3	28.64a	5933.94a	1.15c	26.53b

* Different letters indicate that the Scott-Knott test, at a 5% significance level, showed a significant difference between the means. Mean properties calculated based on five replicates for each treatment.

3.3 Optical properties

Figure 6 illustrates the behavior of the optical properties evaluated in this study, opacity (6a) and transparency (6b). The high transparency is related not only to the nanometric dimensions presented by the nanocelluloses (SIRÓ et al., 2011; HASSAN et al., 2012; BARDET et al., 2013), but also to the greater uniformity of this morphological property (WANG & ZHANG, 2013).

As the CNC content in the nanocomposite formulation increases, average opacity values decrease. Inversely proportional to this decrease, there is an increase in transparency values. Opacity drops by 53% for T3 and 50% and 40% for T2 and T1, respectively. Conversely, as these values decrease, transparency property gains of 6%, 5%, and 4% for T3, T2, and T1, respectively, compared to T0.

Some applications of these nanocomposites in the form of films require a certain opacity, however, for the electronic devices industry, high transparency is advantageous (SIRÓ & PLACKETT, 2010).

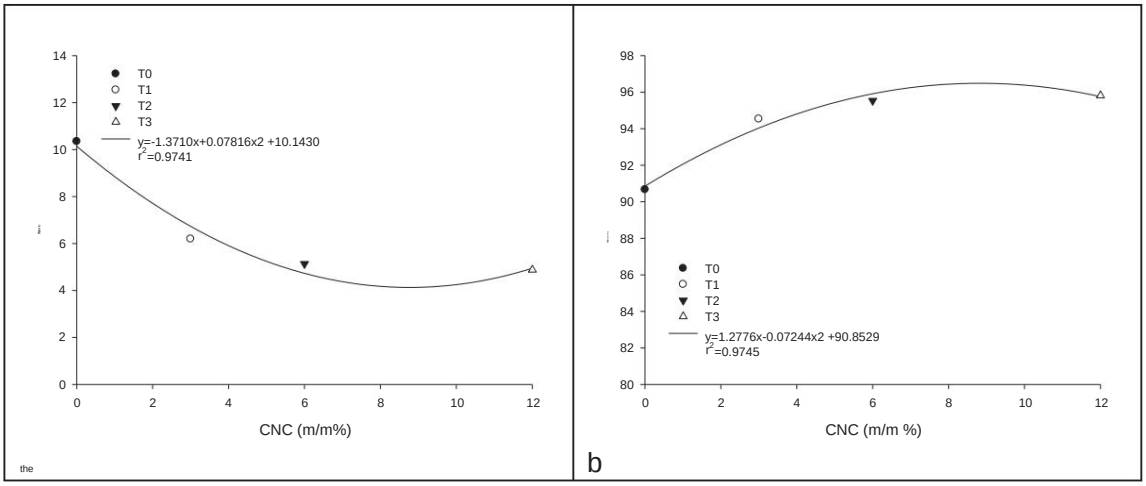

Figure 6 – Behavior of optical properties for the studied treatments, T0 (0% CNC), T1 (3% CNC), T2 (6% CNC) and T3 (12% CNC). a) opacity and b) transparency.

3.4 TGA/DTG

Figure 7 illustrates the thermal behavior and the TGA (Figure 7a) and DTG (Figure 7b) curves. Based on the analysis of the thermal events that occur during the degradation of nanocomposites, they can be divided into three main ones: release of water adhered to the amorphous and surface regions; degradation of the amorphous regions and release of volatiles; and degradation of the crystalline regions and breakdown of the monomers that form the polymer.

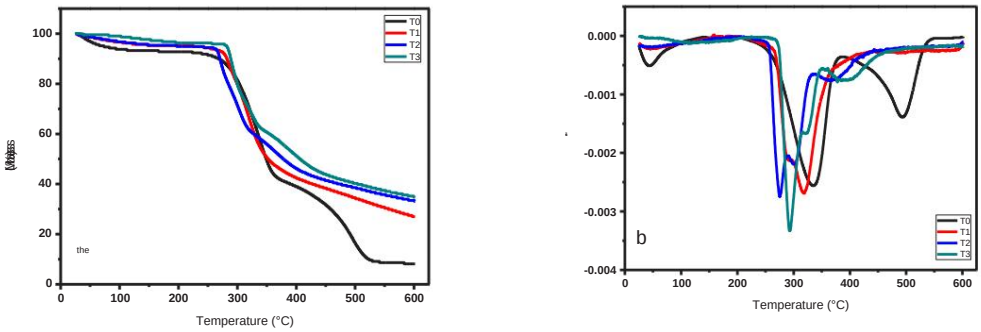

Figure 7 – TGA and DTG thermal degradation behavior curves of nanocomposites CNF-CNC

The first thermal event, which occurred between 30 and 130 °C, can be characterized as the loss of surface moisture or water not chemically bound to the nanostructure. Mandal and Chakrabarty (2014), when evaluating nanocomposites based on polyvinyl alcohol and nanocellulose from sugarcane bagasse, found that water loss occurred in the range of 30 to 140 °C, which is consistent with the data obtained in this work. This thermal event occurs due to the removal of water, which is often adhered only to the surface and requires energy for evaporation, characterizing an endothermic process. Figure 7b shows

It is clear that nanocomposites formed solely by CNF are those that exhibit the characteristics of this first endothermic phase. The hypothesis that this phase is quite evident at T0 is due to the amorphous regions present in the nanostructure, which may be associated with the greater presence of moisture in relation to T1, T2, and T3. According to Randriamantena et al. (2009), this is the so-called thermal stability zone, since it is limited by the initial temperature of thermal degradation of the main wood components. It is worth noting that these components are thermally stable in this temperature range, as long as they are not exposed to heat for prolonged periods (RAAD et al., 2006).

Table 5 – Temperature and mass loss of the main thermal events

Treatment	Peak Temperature (ºC)	Total Mass Loss (%)
T0	330	91
T1	287	73
T2	273	67
T3	265	64

The next two degradation events are responsible for the significant mass loss of the nanocomposites. Teixeira et al. (2010) and Tonoli et al. (2012) observed a decrease in the degradation temperature due to the presence of sulfate groups on the surface of the cellulose nanocrystals (Table 5), which in this study are the constituents of the nanocomposites.
The replacement of OH groups by sulfate groups decreases the activation energy for the degradation of cellulose chains (WANG et al., 2007). The influence of sulfation on nanocrystals can be observed in Figure 7b, where the peaks of the highest mass loss region for the nanocomposites containing 3, 6, and 12% CNC (T1, T2, and T3) are located below 330 °C, while for the nanocomposite containing only CNF, they are at 330 °C. However, when adding cellulose nanocrystals, although the onset temperature of thermal degradation *(Tonset)* decreases due to surface sulfation in CNC, the thermal expansion is lower and therefore the final mass loss is lower as the CNC concentration increases (Table 5). While at T0, 91% of the mass of the nanocomposites is degraded, only 64% of the mass is degraded at T3. However, with the increase in CNC there is greater ash formation.

Thus, the temperature range of 230 to 414 °C characterizes the second thermal event as the one in which the amorphous regions and possible other components such as residual hemicelluloses on the surface are degraded. Hemicelluloses normally present their degradation in the range of 225 to 325 °C and cellulose in the range of 305 to 375 °C, as reported by Prins et al. (2006). The last event in this study was characterized as the degradation of the crystalline regions and the breakdown of the monomers, which for the nanocomposites containing nanocrystals occurred from 325 to 443 °C, while for those containing only CNF it was from 388 to 550 °C.
It should be noted that no event was observed above the temperature of 550 °C. The displacement of the peak of the third degradation event of the nanocomposites at T0 was probably due to the presence of several bonding points between the flexible cellulose nanofibrils, which

because of their high aspect ratio they formed several bonding points and possibly increased the degradation temperature.

Based on the results obtained, it is concluded that the nanocomposites developed in this study have viable thermal stability for various applications, such as in the development of electronic devices, in which temperatures around 150 °C are routine (NOGI et al., 2013)

4. CONCLUSION

The incorporation of CNC into CNF, in the formation of nanocomposites with high mechanical strength and transparency, is a viable technological alternative. The surface topography of the films formed by CNF-CNC nanocomposites is directly influenced by the CNC dosage in the matrix, which promotes different roughness values for the nanofilms produced.
CNF-CNC nanocomposites can be used in food packaging, electronic devices, packaging coatings, and paperboard layers. The CNC dosage in the nanocomposite composition should be determined based on the polymer matrix used for its dispersion and nanofilm formation. Finally, incorporating CNC into the CNF polymer base to form nanocomposites with high mechanical strength and transparency is a viable technological alternative.

REFERENCES

ASTM. (2009). ASTM D 882-09 Standard test method for tensile properties of thin plastic sheeting. West Conshohocken, PA: ASTM International.

ABE, K.; YANO, H. Comparison of the characteristics of cellulose microfibril aggregates of wood, rice straw and potato tuber. Cellulose, vol. 16, no. 6, p. 1017-1023, 2009.

BARDET, R.; BELGACEM, MN; BRAS, J. Different strategies for obtaining high opacity films of MFC with TiO2 pigments. **Cellulose,** vol. 20, no. 6, p. 3025-3037, 2013.

CHUN, S.; LEE, S.; DOH, G.; LEE, S.; KIM, JH Preparation of ultrastrength nanopapers using cellulose nanofibrils. **Journal of Industrial and Engineering Chemistry,** vol. 17, no. 13, p. 521-526, 2011.

DUFRESNE, A. Processing of polymer nanocomposites reinforced with polysaccharide nanocrystals. **Macromolecules,** vol. 15, p. 4111–4128, 2010.

ESPITIA, PJP, SOARES, NFF, TEOFILO, RF, COIMBRA, JSR, VITOR, DM, BATISTA, RA, FERREIRA, SO, ANDRADE, NJ, MEDEIROS, EAA Physical–
mechanical and antimicrobial properties of nanocomposite films with pediocin and ZnO nanoparticles. **Carbohyd Polym,** 94:199-208, 2013.

GEORGE, J.; SREEKALA, MS; THOMAS, S. A review on interface modification and characterization of natural fiber reinforced plastic composites. **Polymer Engineering and Science,** vol. 41, no. 9, p. 1471–1485, 2001.

HABIBI, Y.; LUCIA, LA; ROJAS, OJ Cellulose nanocrystals: chemistry, self-assembly, and applications. **Chemical Reviews,** vol. 110, no. 6, p. 3479-3500, 2010.

HASSAN, ML; MATHEW, AP; HASSAN, EA; EL-WAKIL, AN; OKSMAN, K. Nanofibers from bagasse and rice straw: process optimization and properties. **Wood Sci Technol,** vol. 46, p. 193–205, 2012.

IWAMOTO, S.; NAKAGAITO, AN; YANO, H. Nano-fibrillation of pulp fibers for the processing of transparent nanocomposites. **Applied Physics** A, vol. 89, no. 2, p. 461-466, 2007.

JOSHI, SV; DRZAL, LT; MOHANTY, A.K.; ARORA, S. Are natural fiber composites environmentally superior to glass fiber reinforced composites? **Composite Part** A, v. 35, p. 371–376, 2004.

KHALIL, HPSA; DAVOUDPOUR, Y.; ISLAM, N.; MUSTAPHA, A.; SUDESH, K.; DUNGANI, R.; JAWAID, M. Production and modification of nanofibrillated cellulose using various mechanical processes: A review. **Carbohydrate Polymers,** vol. 99, p. 649– 665, 2014.

LI, X.; TABIL, LG; PANIGRAHI, SD Chemical treatments of natural fiber for use in natural fiber–reinforced composites: A review. **Journal of Polymer Environment,** vol. 15, p. 25–33, 2007.

MANDAL, A.; CHAKRABARTY, D. Studies on the mechanical, thermal, morphological and barrier properties of nanocomposites based on poly(vinyl alcohol) and nanocellulose from sugarcane bagasse. **Journal of Industrial and Engineering Chemistry,** vol. 20, p. 462–473, 2014.

MANOCHA, LM; VALAND, J.; PATEL, N.; WARRIER, A.; MANOCHA, S. Nanocomposites for structural applications. **Indian Journal of Pure and Applied Physics,** vol. 44, p. 135–142, 2006.

NAKAGAITO, AN; FUJIMURA, A.; SAKAI, T.; HAMA, Y.; YANO, H. 2009. Production of microfibrillated cellulose (MFC)-reinforced polylactic acid (PLA) nanocomposites from sheets obtained by a papermaking-like process. **Compos Sci Technol** 69:1293–7, 2009.

NOGI, M. et al. High thermal stability of optical transparency in cellulose nanofiber paper. **Applied Physics Letters,** vol. 102, no. 108, p. 102-106, 2013.

PRINS, MJ; PTASINSKI, KJ; JANSSEN, FJJG Torrefaction of wood. Part 1. Weight loss kinetics. **Journal of Analytical and Applied Pyrolysis,** vol. 77, p. 28–34, 2006.

RAMAZANOV, MA; ALI-ZADE, RA; AGAKISHIEVA, PB Structure and magnetic properties of nanocomposites on the basis PE+Fe3O4 ÿ PVDF+ Fe3O4. **Digest Journal of Nanomaterials and Biostructures,** v. 5, no. 3, p. 727–733, 2010.

RAAD, TJ; PINHEIRO, PCC; YOSHIDA, MI General equation of kinetic mechanisms of carbonization of *Eucalyptus* spp. **Heartwood,** Lavras, v. 12, n. 2, p. 93-106, 2006.

RANDRIAMANANTENA, T.; RAZAFINDRAMISA, FL; RAMANANTSIZEHENA, G.; BERNES, A.; LACABANE, C. Thermal behavior of three woods of Madagascar by thermogravimetric analysis in inert atmosphere. In: **Proceedings of the Fourth High-Energy Physics International Conference,** 2009, Antananarivo, Madagascar.

SEYDIBEYOGLU, MO; OKSMAN, K. Novel nanocomposites based on polyurethane and microfibrillated cellulose. **Composite Science and Technology,** vol. 68, p. 908–914, 2008.

SIRÓ, I.; PLACKETT, D.; HEDENQVIST, M.; ANKERFORS, M.; LINDSTROM, T. Highly Transparent Films from Carboxymethylated Microfibrillated Cellulose: The Effect of Multiple Homogenization Steps on Key Properties. **Journal of Applied Polymer Science,** vol. 119, no. 5, p. 2652–2660, 2011.

SIRÓ, I.; PLACKETT, D. Microfibrillated cellulose and new composite materials: a review. Cellulose, vol. 17, no. 3, p. 459-464, 2010.

TAPPI standard (2006) T220 sp-06, Physical testing of pulp handsheets.

TAPPI standard (2006) T551 om-06, Thickness of paper and paperboard (Soft platen method).

TAPPI standard (2008) T410 om-08, Grammage of paper and paperboard (Weight per unit area).

TAPPI standard (2007) T1214 sp-07, Interrelation of reflectance, R0; Reflectivity, Rÿ; Opacity, C0.89; Scattering, s; and Absorption, k.

Technical association of the pulp and paper industry. **Tappi standard methods.** Atlanta: TAPPI, 2000.

TEIXEIRA, EM; CORRÊA, AC; MANZOLI, A.; LEITE, FL; OLIVEIRA, CR; MATTOSO, LHCCellulose nanofibers from white and naturally colored cotton fibers.
Cellulose, vol. 17, p. 595–606, 2010.

TONOLI, GHD; TEIXEIRA, EM; CORRÊA, AC; MARCONCINI, JM; CAIXETA, LA; PEREIRA-DA-SILVA, MA; MATTOSO, LHC Cellulose micro/nanofibers from Eucalyptus kraft pulp: Preparation and properties. **Carbohydrate Polymers,** v. 89, p. 80– 88, 2012.

TUNC, S., & DUMAN, O. Preparation of active antimicrobial methyl cellulose/

carvacrol/montmorillonite nanocomposite films and investigation of carvacrol release. LWT - **Food Science and Technology,** 44(2), 465–472, 2011.

WANG, H.; LI, D.; ZHANG, R. Preparation of ultralong cellulose nanofibers and optically transparent nanopapers derived from waste corrugated paper pulp. BioResources, vol. 8, no. 1, p. 1374-1384, 2013.

WANG, N.; DING, E.; CHENG, R. Thermal degradation behaviors of spherical cellulose nanocrystals with sulfate groups. **Polymer,** vol. 48, p. 3486–3493, 2007.

YU, L.; DEAN, K.; LI, L. Polymer blends and composites from renewable resources. Program. **Polymer Sci.,** 31(6), 576-602, 2006.

ACKNOWLEDGMENTS

The corresponding author thanks the Brazilian company, a leader in the market pulp sector, for donating the material and the US Department of Agriculture - Forest Products Laboratory for donating nanocrystalline cellulose.